

## Article

# Extreme Tsunami Inundation at Babi Island due to Flores Earthquake Induced Tsunami in 1992

Kyeong Ok Kim<sup>1</sup>, Dong Chule Kim<sup>2</sup>, Jin-Hee Yuk<sup>3</sup>, Efim Pelinovsky<sup>4,5</sup>, and Byung Ho Choi<sup>6\*</sup>

<sup>1</sup>*Marine Radionuclide Research Center, KIOST  
Ansan 426-744, Korea*

<sup>2</sup>*Technology R&D Institute, Hyein E&C Co. Ltd.  
Seoul 157-779, Korea*

<sup>3</sup>*Disaster Management HPC Technology Research Center, KISTI  
Daejeon 305-806, Korea*

<sup>4</sup>*Institute of Applied Physics, Russian Academy of Sciences  
Nizhny Novgorod 603950, Russia*

<sup>5</sup>*Department of Applied Mathematics, Nizhny Novgorod State Technical University n.a. R.E. Alekseev,  
Nizhny Novgorod 603950, Russia*

<sup>6</sup>*Department of Civil and Environmental Engineering, Sungkyunkwan University  
Suwon 440-746, Korea*

**Abstract :** In this paper we investigated the phenomenon of extreme run-up at Babi Island in Indonesia caused by the 1992 Flores earthquake ( $M_w = 7.8$ ) using a series of three-dimensional numerical modeling experiments. Simulations were carried out to investigate how much the presence/absence of the coast of Flores affects the generation of the extreme inundation at Babi Island through the reflection process of tsunami waves.

**Key words :** Flores tsunami, Conical Island, extreme inundation, 3D RANS

## 1. Introduction

A large earthquake with magnitude  $M_w$  7.8 occurred on the north coastal area of the eastern part of Flores Island, Indonesia, at 05:29 GMT (13:29 Flores local time) on December 12, 1992. Most buildings were damaged in Maumere City and its vicinity, where seismic intensity was estimated at 9 to 10 on the Modified Mercalli scale or at 6 on the JMA intensity scale. In the city area, evidence of liquefaction, sand blows, and cracks was observed at many places. The residential area of Wuring village, which is located about 2 km northwest of Maumere on a small sand spit 700 meters long, was hit by the tsunami resulting

in the collapse of 80 percent of the wooden houses and the death of 87 persons of the 1,400 inhabitants. The height of the tsunami was only 2.5-3.2 m above mean sea level. Babi Island, two villages are situated on the south coast of the island; Muslim in the western part and Christian in the eastern, total population of 1,093. All houses were washed away; leaving no trace of buildings. The tsunami took the lives of 263 persons (Choi and Woo 1994; Tsuji and Matsutomi 1993; Yeh et al. 1994; Tsuji et al. 1995). Photos in Fig. 1 are the scenery view taken from the outer sea, showing the destroyed houses and palm trees by tsunami attack in the rear side of Babi Island (taken by Choi of International Tsunami Survey Group).

A field survey of the 1992 Flores Island earthquake tsunami was conducted during December 29, 1992 to

\*Corresponding author. E-mail : bhchoi.skku@gmail.com



(a) the west side of Babi Island (Muslim village)



(b) the east side of Babi Island (Christian village)



(c) Destroyed houses and palm trees by tsunami attack in the rear side of Babi Island

**Fig. 1. Photos in the post field survey (taken by Choi B.H., International Tsunami Survey Group)**

January 5, 1993 along the north coast of the eastern part of Flores Island. International Tsunami Survey Group visited over 40 villages, measured tsunami heights, and interviewed the inhabitants (Tsuji and Matsutomi 1993; Choi and Woo 1994).

Here is summary of the survey results for Babi Island reported by Tsuji et al. (1995). The width of the strait between Babi and Flores Island is about 5 km (Fig. 2). Two villages are situated on the flat land of the southern coast: a Muslim village (Kampungbaru) on the western

side and a Christian village (Pagaraman) on the eastern part. The coral reef is considerably narrower on the south coast, where the two villages are situated, than it is around other parts of the island.

The residential area of the Muslim village, Kampungbaru, faces the sea and a row of palm trees were located along the shore fronting the village. These provided virtually no protection for the houses behind. It measured the runup height by the traces on tree bark. Tsunami height was 3.6 m at the eastern point of the residential area of the Muslim

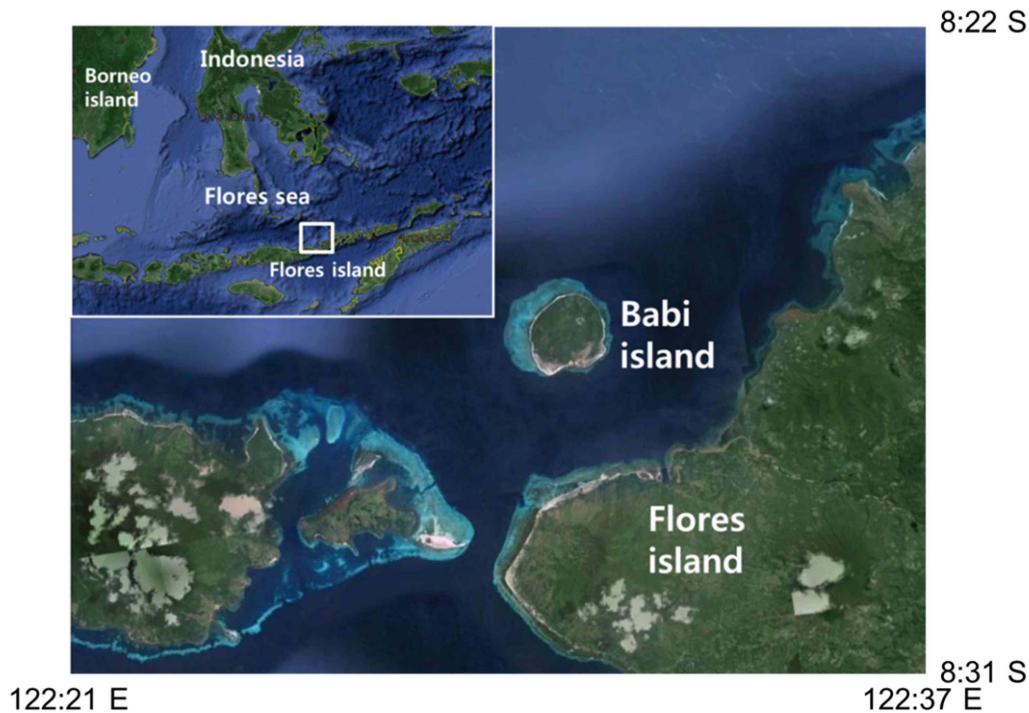


**Fig. 2.** Satellite image of circular Babi Island (2.5 km) diameter, the width of the strait between Babi and Flores Island is approximately 5 km

village. The ground height was only 1.2-2.0 m above mean sea level. Thus, the tsunami with a water thickness of only 2 m entirely washed away the houses. The speed of the sea water is estimated to have exceeded 5 m/s or more. It also measured the tsunami height at 7.2 m at two points on the foot of the steep mountain slope behind the palm tree forest, west of the residential area. The height of 7.2 m can be explained as a doubling of the height due to a reflected wave. Some witnesses indicated that the waves originated from the south, which would suggest that the waves which reflected from the mainland of Flores Island affected Babi Island more seriously than the direct waves from the source.

The Christian village, Pagaraman is located on the southeast coast of Babi Island, directly facing Nebe village on the mainland of Flores Island. All houses in this village were swept away, and only foundations remained. Most of the residential area was surrounded by a palm tree forest, and the materials of the houses were carried into the forest. It could clearly trace the inundation height on the surface of palm trees and measured it as 5.6 m. Sea water surged across the dune and flowed westward along the valley behind. The ground height of the residential area was about 2 m, thus the thickness of sea water can be estimated as about 3 m.

It reported that maximum runup height of Muslim village area in the south western part of the Babi Island was 7.14 m and 7.15 m at two points on the foot of the steep mountain slope behind the palm tree forest, west end of the residential area. And maximum runup height of Christian village area in the south eastern part of the Babi Island was 5.6 m. Fig. 3 shows that measurement results by Tsuji et al. (1995) of runup heights plotted on the Google-earth satellite image at each measured point locations – some points moved inland because they have some mismatches the measured points with sketched map.

According to the surveying results, at the circular shaped Babi Island unexpectedly large tsunami inundations in the lee of the small island were observed and huge human and material losses were incurred (Liu et al. 1991; Liu et al. 1995a, b; Cho 1995; Tsuji and Matsutomi 1993). Motivated by the catastrophe in Babi Island, Indonesia (Yeh et al. 1994), during the 1992 Flores Island tsunami, laboratory experiments were performed in a large-scale basin at the Coastal and Hydraulics Laboratory (hereinafter referred as CHL), US Army Corps of Engineers (Briggs et al. 1994). This laboratory results were provided as benchmark problem of runup simulations and a series of numerical experiments were reported using various numerical schemes however model applications were





**Fig. 3. The locations of the field measurement by Tsuji et al. (1995) and tsunami heights (in metres) plotted on the satellite image**

limited to two-dimensional. Among these model simulations, Liu et al. (1995a, b) and Cho and Liu (1999) developed a numerical model based on the two-dimensional nonlinear shallow-water equations to describe the propagation and runup of solitary waves. Obtained results agreed well with laboratory measurements carried out by CHL.

Choi et al. (2007) applying the 3D RANS model to simulate wave runup on conical island. In the runup computation, 3D calculations are in very good comparison with laboratory and 2D numerical results. From the numerical results and comparison with the experimental measured data, reproduce the following results. From the 3D model, the horizontal velocity is strongly dependent on the water depth especially at the lee side of the island. A strong vertical velocity profile is observed near the conical island and these patterns persist beyond the island. Strong turbulent energy dissipation is shown on the lee side, which implies intense energy transfer from the wave to the land. This could explain why the 3D model has stronger horizontal velocity than the 2D, but has similar runup height as the 2D. The location at which the maximum TKE is generated is not in the lee, but both lee-side edges of the Island. From these conclusions, it can be argued that there is an obvious limitation on using depth-averaged 2D models for the simulation of runup processes on the conical shape island. The 3D numerical results eventually

need to be compared with the physical experimental data, especially for flow pattern and turbulent intensity values.

In this study, it will be shown that the presence of Flores Island acts as an additional mechanism to the extreme inundation at the Babi Island comparing with the idealized conical island simulation by Choi et al. (2007). Numerical simulations with real topography have been made, as a sequel to the previous idealized conical island simulation by Choi et al. (2007), to investigate the phenomenon of extreme runup at the Babi Island when 1992 Flores tsunami occurred. Simulations have been carried out to investigate how much the presence of the coast of Flores affects the generation of the extreme inundation at the Babi Island through the reflection process of tsunami waves, comparing results in the presence/absence of the coast of Flores.

3D RANS model was employed to reproduce the tsunami wave characteristics in the near shore tsunami around a circular shaped Babi Island. The wave field in the coastal area was modeled within the framework of fully nonlinear dispersive Reynolds-averaged Navier-Stokes (RANS) equations solved using the FLOW3D code. Boundary conditions for this model were extracted from computed wave characteristics obtained from the tsunami propagation model based on the hydrostatic hydrodynamic model (Malhadas et al. 2009).



## 2. Hydrostatic Tsunami Propagation Model Simulation

The tsunami propagation model has a multi-nesting system with a grid resolution from 900 m to 50 m, with the initial water elevation calculated using Okada's solution. The hydrostatic finite volume model (Braunschweig et al. 2004) was applied to simulate tsunami wave propagation during the 1992 Flores Tsunami event. Three sub-regions, which all had different grid sizes with 10 vertical sigma levels, were used in the tsunami propagation model. A radiation open-boundary scheme was used in the first domain (D1), and a one-way nesting scheme was used for the other domains by interpolating the water elevation and current values from the mother domain. Also the other smaller domain (D4) was prepared to inundation simulation using RANS model.

Fig. 4 shows the 4 domains of the numerical simulation with the one-way nesting system. The largest domain (D1) has a  $360 \times 360$  mesh system with a grid resolution of 30 seconds (approximately 900 m) and a time step of 1 sec. The sub-domains are nested using 1:3 and 1:5 grid

interpolations. The second and third domains have the  $390 \times 300$  and  $450 \times 360$  mesh systems with the grid resolutions of 10 and 2 seconds. The "land" boundary conditions were assumed to be fully reflected in last sea grids in D1, with a minimum water depth of 10 m. The inundation of tsunami waves in domains D2 and D3 was computed using the wet-and-dry scheme proposed by Martins et al. (2001). The topography and bathymetry data are composed by GEBCO (Jones 2003) and ASTER (Abrams et al. 2002) at 1 arc-second resolution with the modification using the bathymetry chart used in Choi and Woo (1994). Because detailed topography data for the Babi Island is not available, various photographs from the survey reports (Choi and Woo 1994; Tsuji and Matsutomi 1993; Yeh et al. 1994; Tsuji et al. 1995) and satellite images from Google Earth were used to modify the land elevation of the island. Fig. 5 shows the bathymetry of the third domain (D3). Table 1 also shows the information for the grid and nesting systems in all domains.

Fig. 6 shows the total vertical component of water deformation computed using Okada's solution (1985) with the fault parameters of Flores Island Earthquake

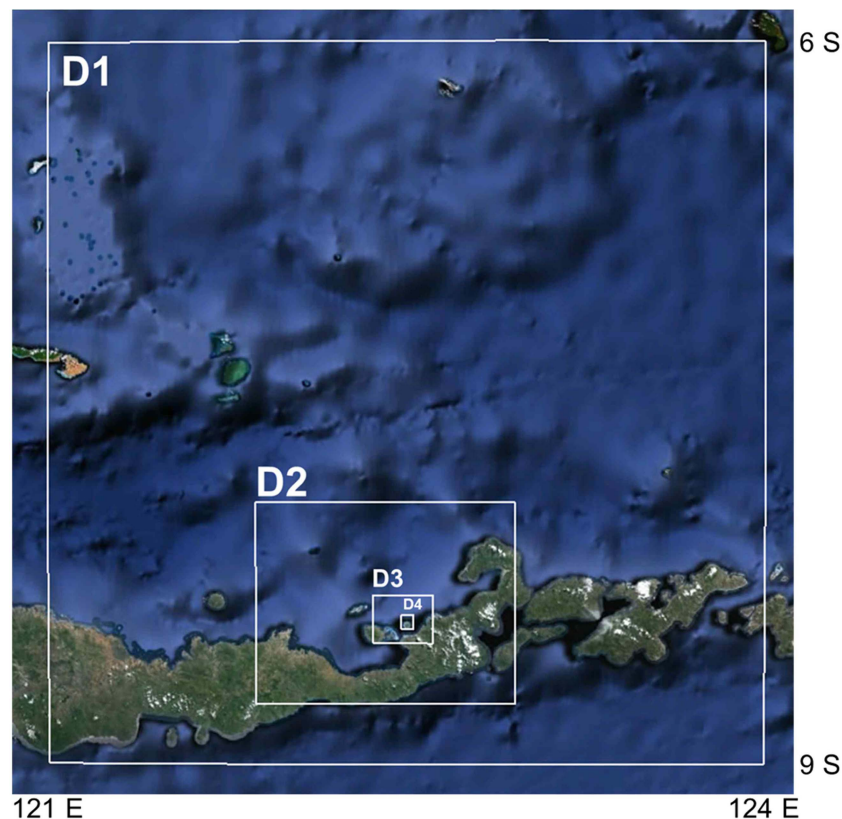


Fig. 4. Computation domains of the tsunami propagation model (Braunschweig et al. 2004) for the Indonesia Flores tsunami, 1992

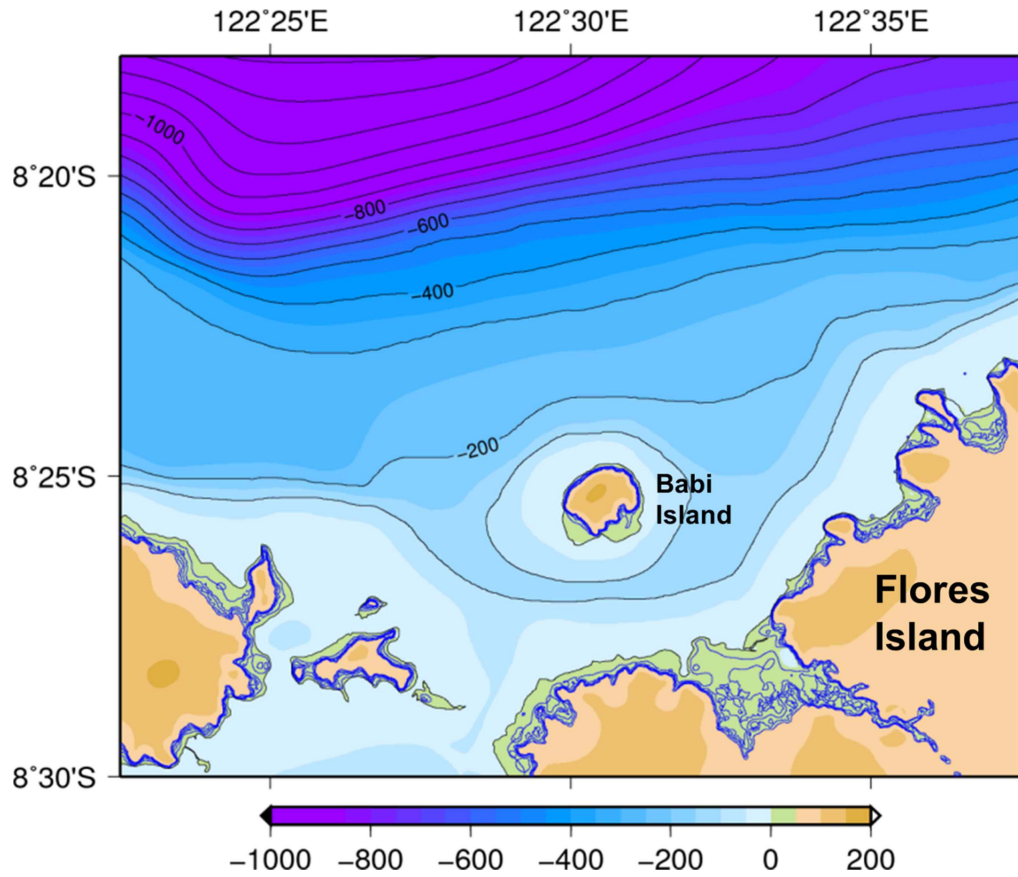


Fig. 5. The bathymetry of the third domain (D3). The black contours indicate the water depth with 100 meter intervals, and the blue contours on green area indicate the land height with 10 meter intervals under 50 meter land height

Table 1. Information of the grid and nesting systems

Domain	NX	NY	NZ	DX DY (arc-sec)	DT (sec)	Nesting ratio	Computation mode
D1	360	360	10 $\sigma$	30	1.0		3D
D2	390	300	10 $\sigma$	10	1.0	1:3	3D Wet-Dry
D3	450	360	10 $\sigma$	2	0.2	1:5	3D Wet-Dry
D4	650	640	95 z	0.4 (10 m)	Flexible	1:5	3D RANS

(Imamura et al. 1995; Table 2). The initial velocity is assumed to be zero. The water deformation ( $\Delta U$ ) is composed of the vertical displacement ( $U_z$ ) and the vertical movement ( $Uh$ ) converted by horizontal movement ( $U_x$ ,  $U_y$ ) at the bottom ( $H$ ) slope.

$$\Delta U = U_z + Uh$$

$$Uh = -U_x \frac{\partial H}{\partial x} - U_y \frac{\partial H}{\partial y}$$

The computed tsunami wave heights for domains 1 to 3 were compared with the observed heights (Fig. 7). The red dots in the lower figure indicate the survey locations, and the red dots in the upper figure indicate the observed tsunami runup heights. The yellow, green and blue dots in the upper figure indicate the computed maximum water elevations in D1, D2 and D3. Because of the low resolution of model, the good comparison was not shown. Especially the maximum water elevations of D1 were significantly underestimated.

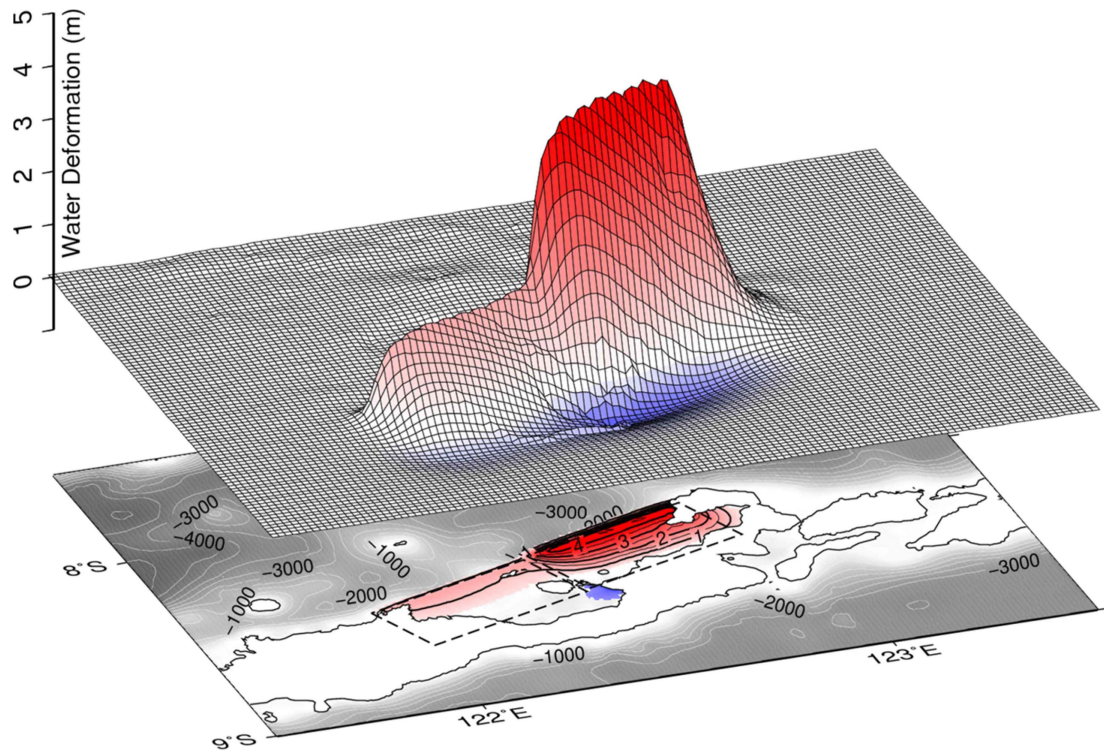


Fig. 6. The vertical component of water deformation (meters) computed by Okada's solution (1985)

Table 2. Fault parameters of the Flores Island Earthquake based on the fault model of Imamura et al. (1995)

Subfault	Latitude (°S)	Longitude (°E)	Length (km)	Width (km)	Depth (km)	Rake	Strike	Dip	Slip (cm)
A	8:27:00	121:55:48	50	25	3	64	70	32	320
B	8:16:48	122:22:12	50	25	3	64	70	32	960

### 3. Non-hydrostatic Tsunami Inundation Model Simulation

Non-hydrostatic RANS 3D model was employed to reproduce the tsunami wave characteristics in the near shore tsunami around a circular island and the extreme inundation on the valley belong to the island. The wave field in the coastal area was modeled within the framework of fully nonlinear dispersive Reynolds-averaged Navier-Stokes (RANS) equations solved using the FLOW3D code. Open boundary conditions for this model were imposed by extracting representative values of sea surface elevation and three-dimensional velocities ( $u$ ,  $v$ ,  $w$ ) from the results of tsunami propagation model based on the hydrostatic hydrodynamic model (Malhadas et al. 2009), assuming that the horizontal variation of the variables along the open boundary is small (note that FLOW3D in fact accepts only a single time-dependent value for each

variable). The no-slip condition is imposed at the sea bottom. No motion is initially assumed in this study. At the outset it is worth commenting the influence of initial conditions on the occurrence of phase delay in FLOW3D results, comparing with the hydrostatic model results. Unlike other situations values of the initial tsunami wave heights are non-zero on the incident boundary and within the model domain near the incident boundary because the source is located at the nearby place. Preliminary calculations therefore showed that the cold start simulation using FLOW3D lags 30 seconds behind the hydrostatic model results. However, the phase discrepancy does not cause a serious problem in this study because the present study is mainly concerned with the occurrence of extreme runup heights and their processes.

Experiments have been carried out in order to investigate such as reflection, diffraction, and propagation. The tsunami wave diffracted by Babi Island made the effect of



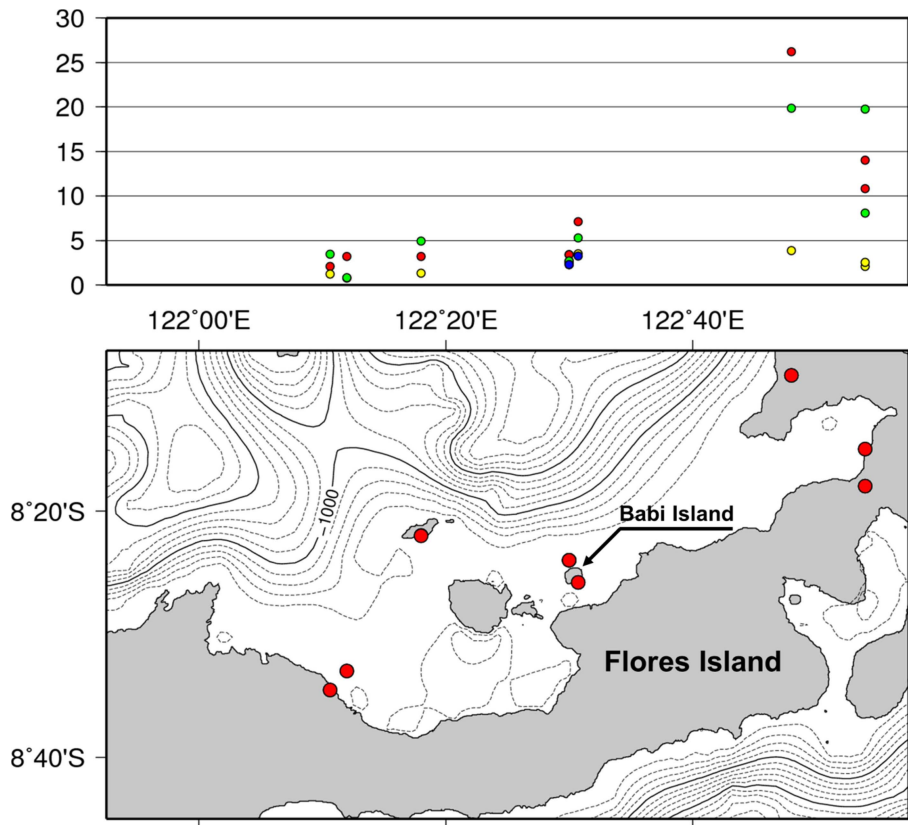


Fig. 7. The lower figure shows the survey locations in the red dots. The upper figure shows the observed tsunami heights (red dots) and the computed maximum water elevations (D1: yellow dots, D2: green dots, D3: blue dots) using hydrostatic model

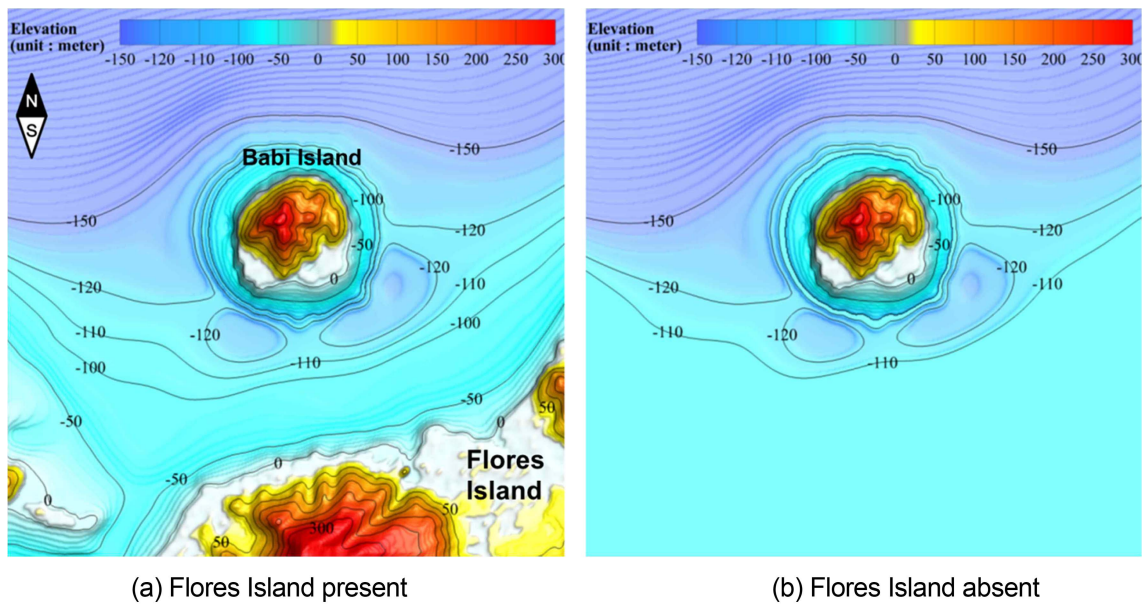


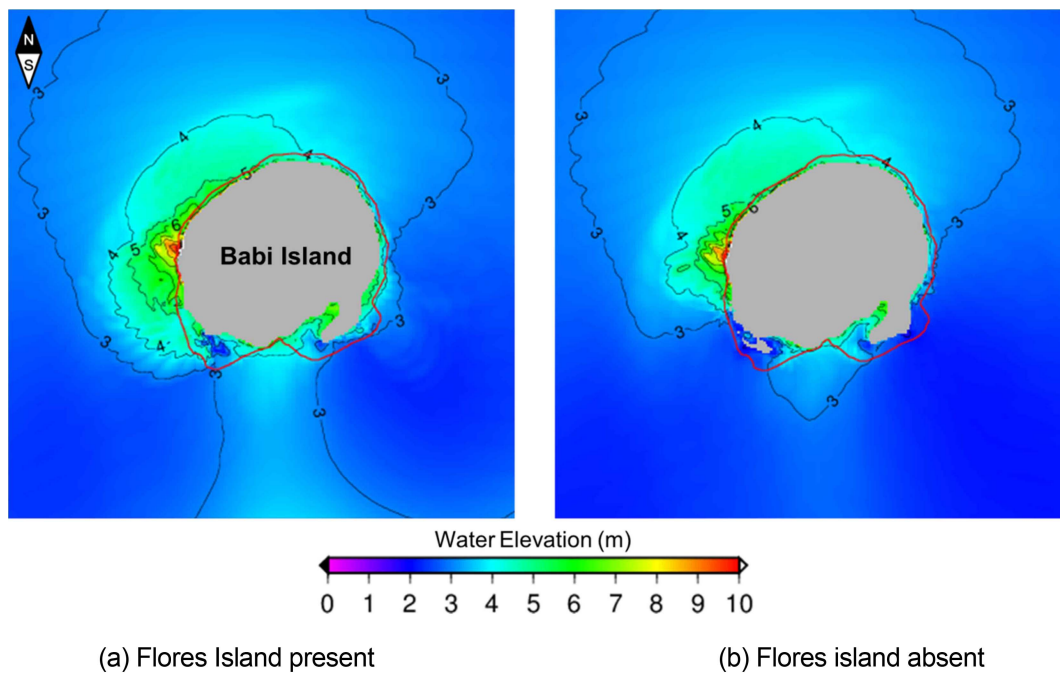
Fig. 8. Topography and bathymetry of the Flores Island present case (left) and absent case (right) for 3 dimensional non-hydrostatic simulations

propagation delay for the Flores Island - present and absent condition located behind (southward) the Babi Island, and this affected to Babi Island inundation. Fig. 8 shows that topography and bathymetry of two different cases described above for 3 dimensional simulations. Left panel indicates Flores island present case (real condition) and right panel indicates Flores island absent (removed above -110 m as elevation) case.

It reported that maximum runup height of Muslim village area in the south western part of the Babi Island was 7.14 m and 7.15 m at two points on the foot of the

steep mountain slope behind the palm tree forest, west end of the residential area. And maximum runup height of Christian village area in the south eastern part of the Babi Island was 5.6 m. Both villages were completely destroyed by the tsunamis, and almost all houses and evidence of the village was washed away (Choi and Woo 1994; Tsuji and Matsutomi 1993; Yeh et al. 1994; Tsuji et al. 1995).

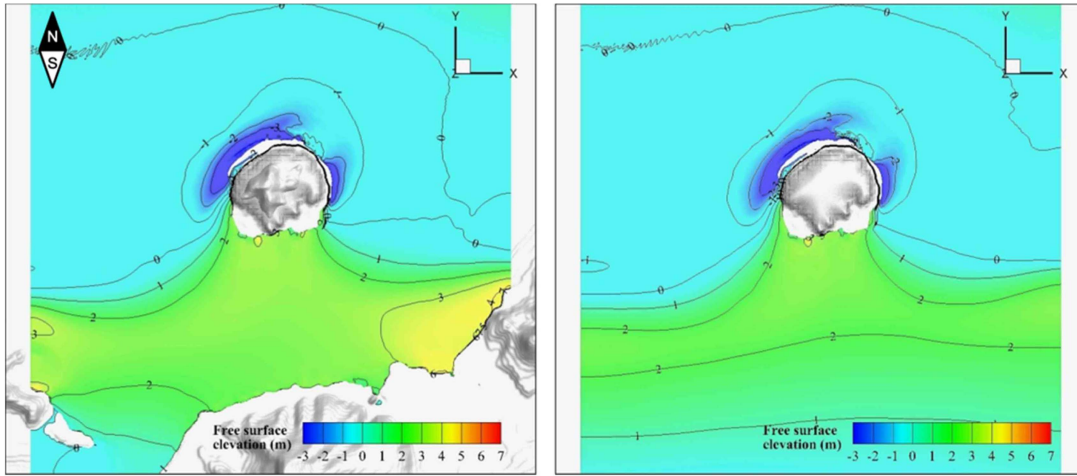
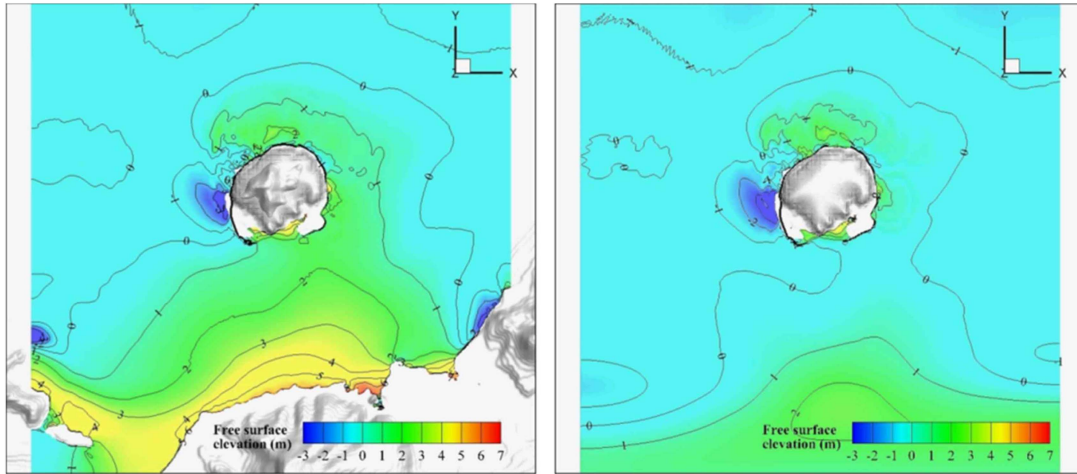
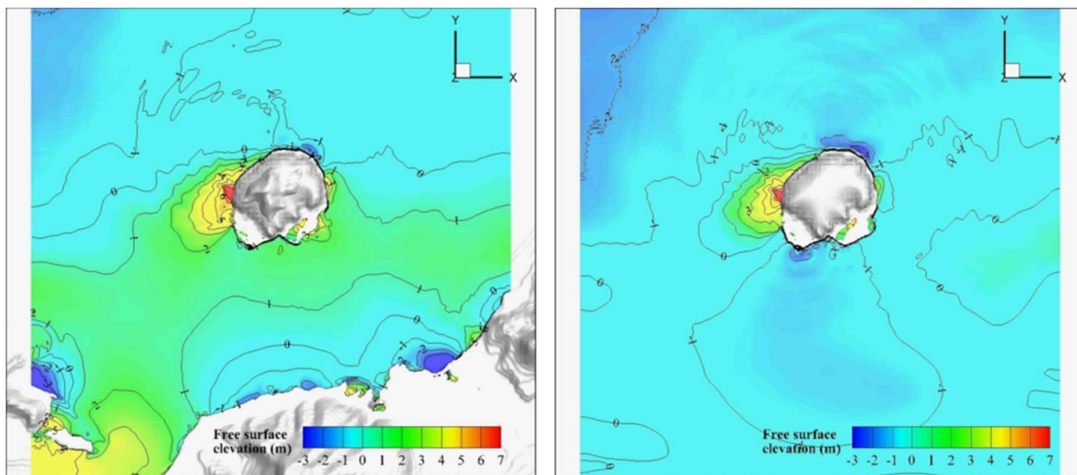
The extreme inundation of tsunami waves at Babi Island were reproduced by numerical simulation using a CFD model solving the Reynolds-averaged Navier-Stokes (RANS) equations. Comparison of computational results



**Fig. 9. Computed maximum runup height distribution for the cases Flores Island is present (a) and Flores Island absent (b). The red lines indicate the original coastline**

**Table 3. List of the measured tsunami heights corrected to the measured time from mean sea level (MSL). The accuracy of heights of most of the points is estimated to be 0.1 m (Tsuji et al. 1995). And it's comparison with measured and computed values in cases of Flores Island present and absent**

Location (Babi Island)	GPS measurement location		Tsunami height above MSL (m)	Computations	
	Latitude (°S)	Longitude (°E)		Present	Absent
Muslim V-1	8:26:06.0	122:30:21.0	3.57	3.80	3.20
Muslim V-2	(Valley of western end)		7.14	7.10	6.80
Muslim V-3	(40 m west of V-2)		7.15	7.20	6.90
Christian V-D	8:25:45.7	122:30:50.0	5.63	5.80	5.30
Christian V-E	8:25:44.8	122:30:48.4	5.42	5.50	5.20
Christian V-F	8:25:42.2	122:30:50.3	4.57	5.30	5.20
Christian V-G			4.08		
Christian V-H			4.00		

(a)  $t = 360$  sec(b)  $t = 450$  sec(c)  $t = 540$  sec

**Fig. 10.** Free surface elevation contour computed for the cases Flores Island is present (left panel) and absent (right panel)



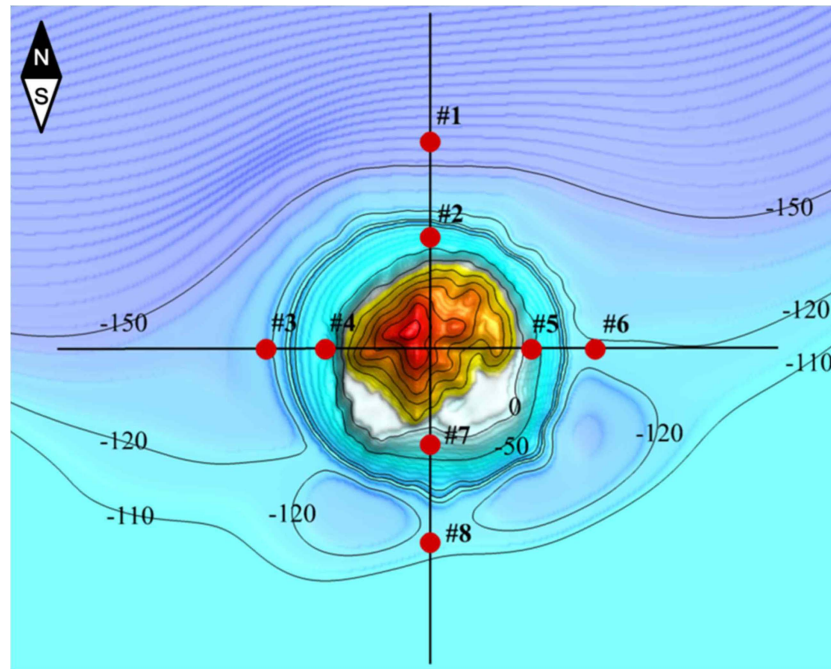


Fig. 11. Location map of the comparing points for free surface elevation variation on time

in the presence/absence Flores Island which is located south of the Babi Island is described below.

The inundation results by the numerical simulations were compared with the field measured runup heights in cases of the Flores Island is present behind (southward) Babi Island condition and absent. The case of the Flores Island is present showed the good agreement with measurement than the absent case. The measured maximum runup height of Muslim village at the west end was 7.15 m while computational height is 7.2 m. At the Christian village, the measured maximum runup height was 5.6 m and computed one is 5.5-6.0 m (Fig. 9(a) and Table 3). As nearly same field investigation report as numerical simulation reproduced both villages were completely inundated. Fig. 9 shows that computed maximum runup height distribution by the numerical simulation for the Flores Island present. The red lines indicate the original coastline. As shown in propagation model results (Fig. 7), maximum runup heights of the Babi island is 5 m or below at the domain D2 and D3. It concerned that three-dimensional model can reproduce complex tsunami inundation phenomenon more accurately on the specific local site such as circular shaped Babi Island on this study than tsunami propagation model.

In case of the Flores Island absent condition, the maximum measurement runup height of Muslim village at the west end was 7.15 m while computational height is

6.9 m. At the Christian village, the measured maximum runup height was 5.6 m and computed height is 4.0-5.5 m. It was underestimated with computational result as measured runup height and Flores Island present case's result about 0.5-1.5 m (Fig. 9(a) and Table 3). As not same field investigation report as numerical simulation have not reproduced both villages were completely inundated, especially not fully inundated in the Muslim village. Fig. 9(b) shows that computed maximum inundation distribution by the numerical simulation for the Flores Island absent case.

Fig. 10 shows that free surface elevation on contour for the Flores Island present case (left) and absent case (right) at 3D computation full area. Fig. 11 shows that location map of the comparing points for free surface elevation variation on time. And Fig. 12 shows that free surface elevation variation on time for the Flores Island present and absent case (No. 1 to 8). It can be shown that point 1, 2, 3, 4, 5, 6 (in front and lee side of Babi Island) similar to each other case about 350 sec before and some variation is shown after 350-400 sec. But point 7 and 8 (back side of Babi Island) especially shows that maximum tsunami wave height occurred at 400 sec at each case and in the Flores Island absent case, wave height rundown suddenly but the Flores Island present case, wave height slowly rundown. In this feature related to runup and inundation process on the Babi Island. Flores Island affects tsunami

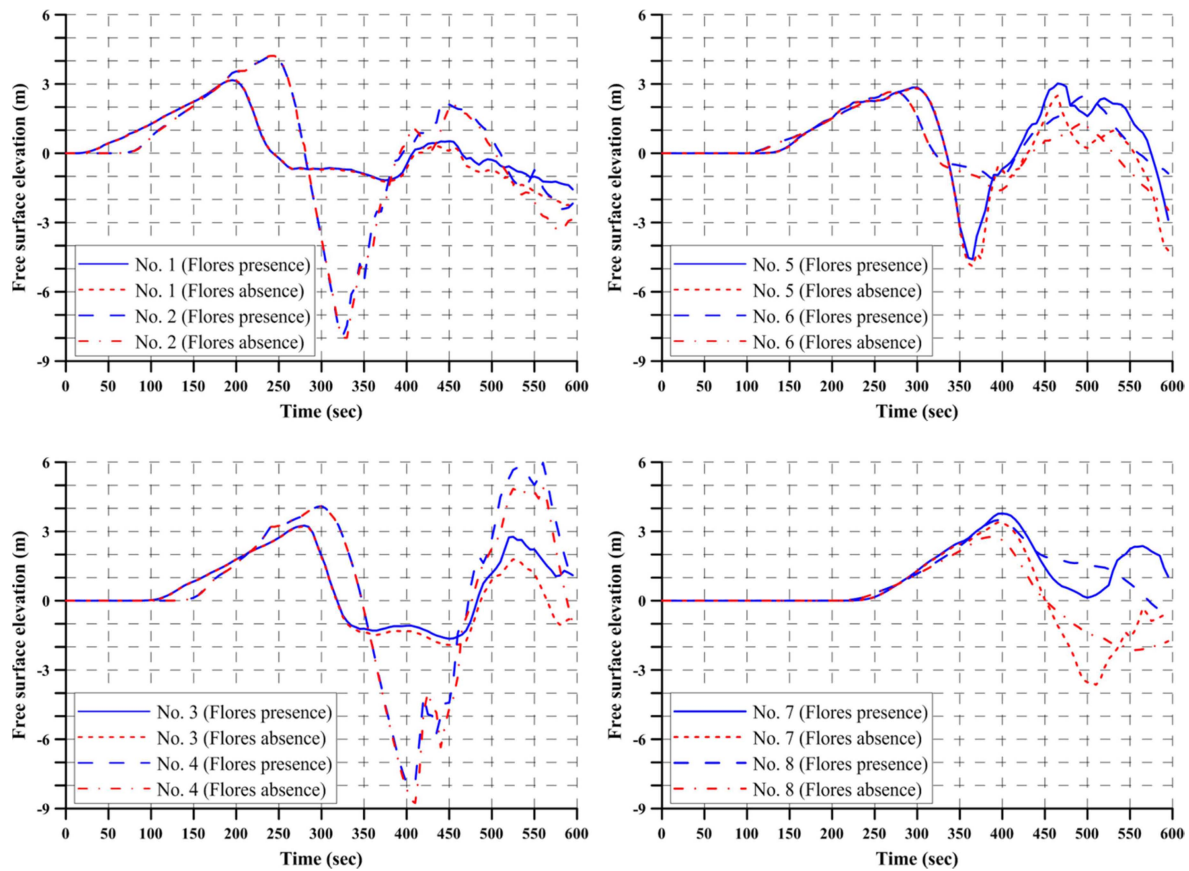


Fig. 12. Free surface elevation variation on time for the cases Flores Island is present and absent

wave propagation time, it can be shown that Flores Island present case's tsunami wave diffracted by Babi Island propagated slowly rather than Flores Island absent case. It was mentioned that fully inundation or not at the Muslim village and more good comparison results for measured tsunami heights for the Flores Island present case as the Figs. 9, 10 and Table 3.

Fig. 13 shows the distribution of computed vertical velocity in the perspective front view. The strong vertical velocity of attaching tsunami wave in the north of Babi Island is shown. The area for the post tsunami investigation was limited to two villages of the south area of Babi Island where many people were killed. It presented that numerical simulation results in the rear side of Babi Island, tsunami had not generated strong vertical velocity because south coasts have the mild slope beach and land topography. Fig. 14 shows the free surface around Babi Island at different times on laid-top view. It can well be shown tsunami wave propagation, runup and inundation process on the Babi Island.

#### 4. Conclusion

The reported maximum runup height of Muslim village area in the south western part of the Babi island was 7.14 m and 7.15 m at two points on the foot of the steep mountain slope behind the palm tree forest, west end of the residential area. And maximum runup height of Christian village area in the south eastern part of the Babi Island was 5.6 m. Both villages were completely destroyed by the tsunamis, and almost all houses and evidence of the village was washed away (Choi and Woo 1994; Tsuji and Matsutomi 1993; Yeh et al. 1994; Tsuji et al. 1995).

In case of the Flores Island present behind the Babi island, numerical simulation inundation results have good agreement with measurement, reproducing the complete inundation of villages as in the field investigation report. On the while, the computation underestimated runup heights in case without Flores Island. It was also found that the presence of Flores Island affects tsunami wave propagation time; the diffraction caused by Babi Island

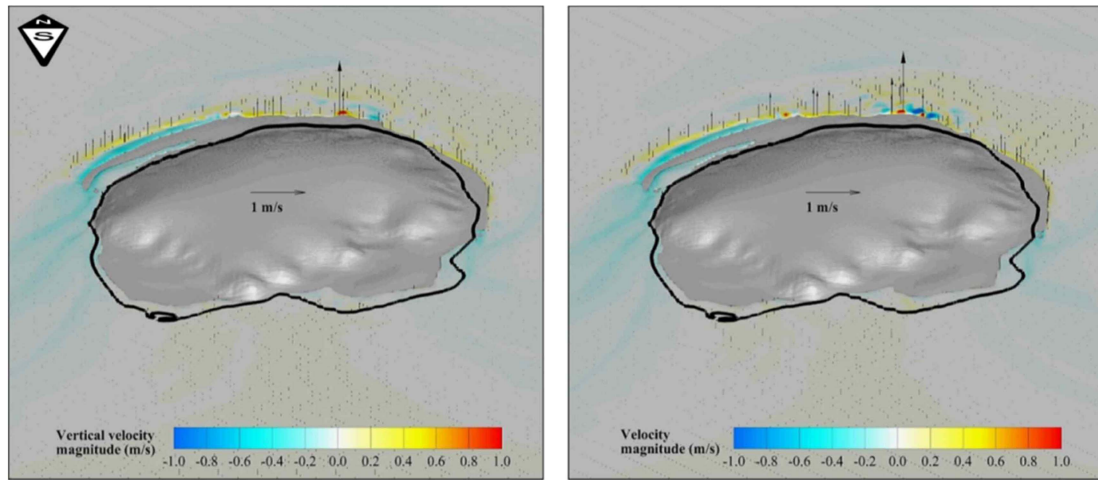
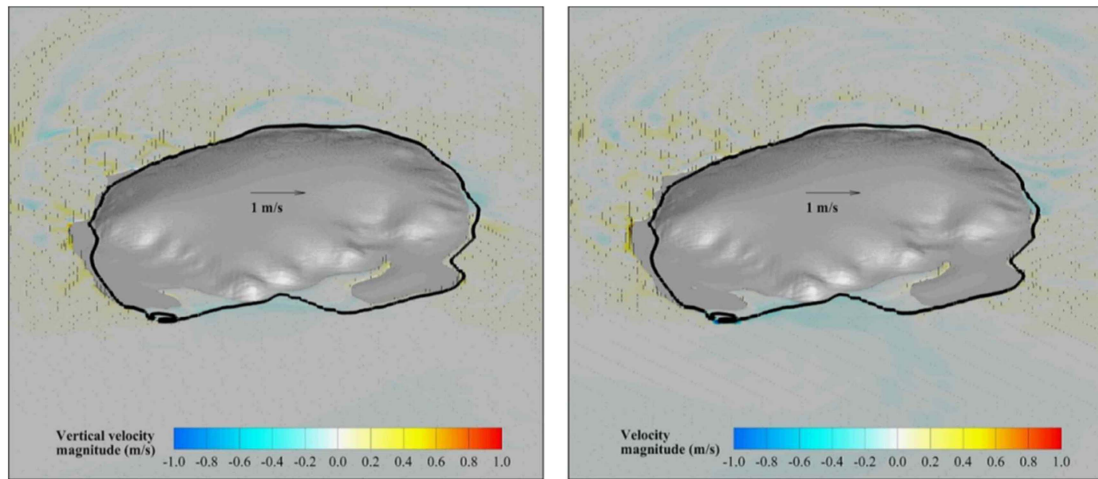
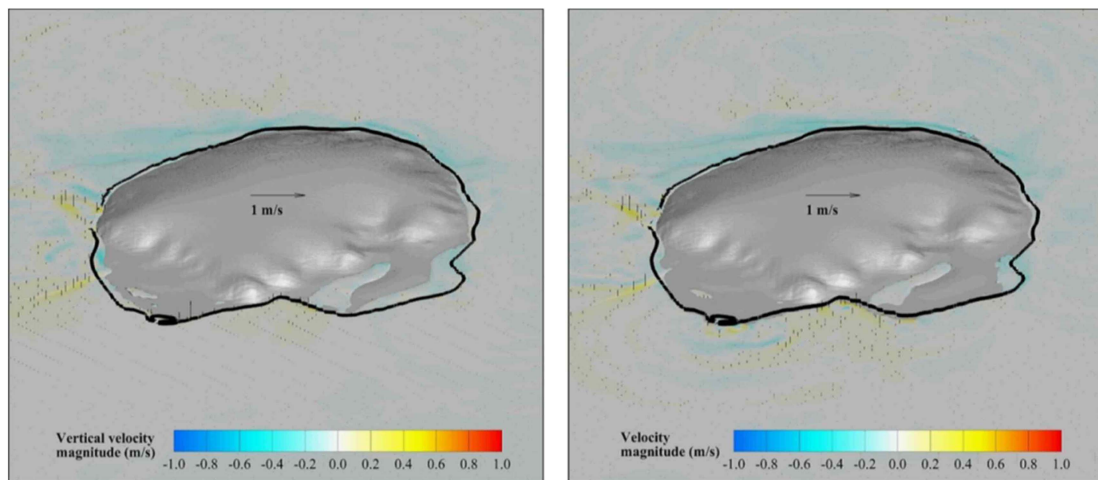
(a)  $t = 360$  sec(b)  $t = 450$  sec(c)  $t = 540$  sec

Fig. 13. Vertical velocity vector field (vertical velocity magnitude on contour) computed for the cases Flores Island is present (left) and absent (right) in the perspective front view



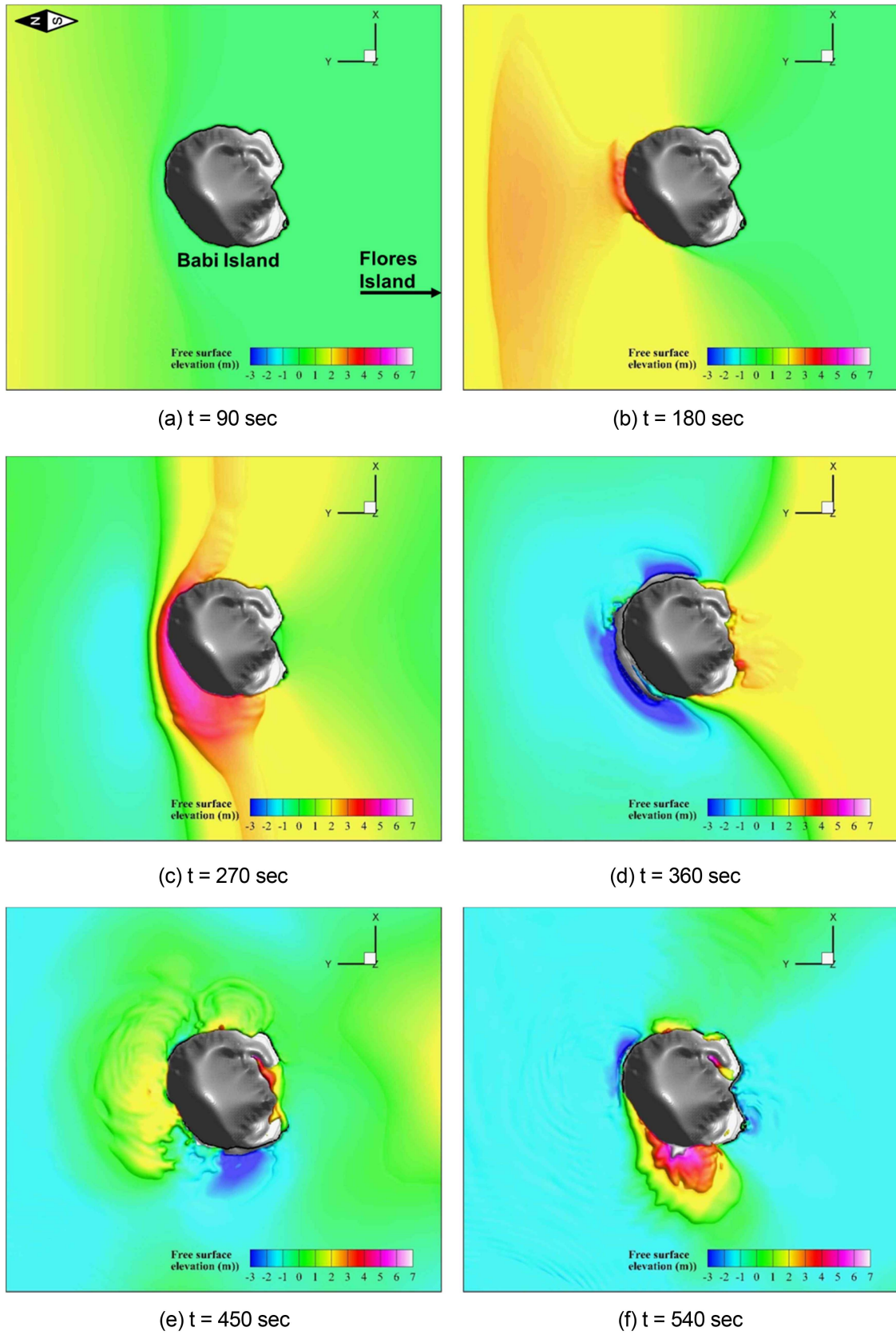


Fig. 14. Snapshots of free surface around Babi Island at different times in laid-top view

retarded the wave propagation, resulting in good reproduction of measured tsunami heights. Computed vertical velocity distribution in the north Babi island is stronger than that of the south area of Babi Island where post-investigation was focused due to the huge death toll. Numerical simulation generated no strong vertical velocity on the rear side of Babi Island because the south coast has beach and land topography with mild slope.

The three-dimensional model developed for the Babi Island due to Flores earthquake tsunami in 1992 will be used a basic tool for the more practical and realistic analysis such as estimation of extreme runup heights, and simulation of breaking and inundation processes associated with the attack of disastrous tsunami or storm surge to the coastal structures of the sea port and power plants, and coastal city areas. Furthermore, it is expected to use the model in providing the information for the coastal evacuation plan.

## Acknowledgements

This study was supported by the China-Korea cooperative research project funded by CKJORC and MOF as well as a major project titled the development of essential technologies for the response of the marine radioactivity impact prediction system funded by KIOST, and the project for the development of HPC-based management system against national-scale disaster by KISTI. EP thanks State Contract No.2014/133.

## References

- Abrams M, Hook SJ, Ramachandran B (2002) ASTER User Handbook - Version 2. Jet Propulsion Laboratory, 135 p
- Braunschweig F, Chambel P, Fernandes L, Pina P, Neves R (2004) The object-oriented design of the integrated modelling system MOHID. In: Computational methods in water resources international conference. North Carolina, USA, 13-17 June 2004, pp 1079-1090
- Briggs MJ, Synolakis CE, Harkins GS (1994) Tsunami runup on a conical island. In: International symposium : waves - physical and numerical modelling. Vancouver, Canada, 21-24 August 1994, pp 446-455
- Cho YS (1995) Numerical simulations of tsunami propagation and runup. Ph.D. Thesis, Cornell University, NY
- Cho YS, Liu PL-F (1999) Crest length effects in nearshore tsunami run-up around islands. *J Geophys Res* **104**(C4): 7907-7913
- Choi BH, Woo SB (1994) Computation of Tsunamis of the 1992 Flores Island Earthquake. *J Korean Soc Coast Ocean Eng* **6**(1):109-116 (in Korean)
- Choi BH, Kim DC, Pelinovsky E, Woo SB (2007) Three-dimensional simulation of tsunami run-up around conical island. *Coast Eng* **54**:618-629
- Imamura F, Gica E, Takahashi T, Shuto N (1995) Numerical simulation of the 1992 Flores tsunami: interpretation of tsunami phenomena in northeastern Flores Island and damage at Babi Island. *Pure Appl Geophys* **144**(3-4): 555-568
- Jones MT (2003) GEBCO Digital Atlas: centenary edition of the IHO/IOC general bathymetric chart of the oceans. National Environmental Research Council, Swindon, UK
- Liu PL-F, Synolakis C, Yeh H (1991) A report on the international workshop on long wave runup. *J Fluid Mech* **229**:678-688
- Liu PL-F, Cho YS, Briggs MJ, Kanoglu U, Synolakis CE (1995a) Runup of solitary waves on a circular island. *J Fluid Mech* **302**:259-285
- Liu PL-F, Cho YS, Yoon SB, Seo SN (1995b) Numerical simulations of the 1960 Chilean tsunami propagation and inundation at Hilo, Hawaii. In: Tsuchiya Y, Shuto N (eds) *Tsunami: progress in prediction, disaster prevention and warning*. Kluwer Academic Publishers, pp 99-115
- Malhadas MS, Leitão PC, Silva A, Neves R (2009) Effect of coastal waves on sea level in Óbidos Lagoon, Portugal. *Cont Shelf Res* **29**(9):1240-1250
- Martins F, Neves RJ, Leitão PC, Silva AJR (2001) 3-D modelling in the Sado estuary using a new generic coordinate approach. *Oceanol Acta* **24**:51-62
- Okada Y (1985) Surface deformation due to shear and tensile faults in a half-space. *Bull Seismol Soc Am* **75**:1135-1154
- Tsuji Y, Matsutomi H (1993) Damages due to the Tsunami. Report of the field survey on the flores island earthquake-tsunami of December 12, 1992. Report Grant in Aid, No. B-4-4, pp 70-87 (in Japanese)
- Tsuji Y, Matsutomi H, Imamura F, Takeo M, Takeo M, Kawata Y, Matsuyama M, Takahashi T, Sunarojo, Harjadi P (1995) Damage to coastal villages due to the 1992 Flores Island earthquake tsunami. *Pure Appl Geophys* **144**(3-4):481-524
- Yeh H, Liu PL-F, Briggs M, Synolakis CE (1994) Propagation and amplification of tsunamis at coastal boundaries. *Nature* **372**:353-355

Received Jan. 5, 2015

Revised Feb. 6, 2015

Accepted May 14, 2015